

A Physical Model for the Co-evolution of QSOs and of their Spheroidal Hosts

Gian Luigi Granato^{1,2}
granato@pd.astro.it

Gianfranco De Zotti^{1,2}
dezotti@pd.astro.it

Laura Silva³
silva@ts.astro.it

Alessandro Bressan^{1,2}
bressan@pd.astro.it
and

Luigi Danese²
danese@sissa.it

ABSTRACT

We present a physically motivated model for the early co-evolution of massive spheroidal galaxies and active nuclei at their centers. Within dark matter halos, forming at the rate predicted by the canonical hierarchical clustering scenario, the gas evolution is controlled by gravity, radiative cooling, and heating by feedback from supernovae and from the growing active nucleus. Supernova heating is increasingly effective with decreasing binding energy in slowing down the star formation and in driving gas outflows. The more massive proto-galaxies virializing at earlier times are thus the sites of the faster star-formation. The correspondingly higher radiation drag fastens the angular momentum loss by the gas, resulting in a larger accretion rate onto the central black-hole. In turn, the kinetic energy carried by outflows driven by active nuclei can unbind the residual gas, thus halting both the star formation and the black-hole growth, in a time again shorter for larger halos. For the most massive galaxies the gas unbinding time is short enough for the bulk of the star-formation to be completed before type Ia supernovae can substantially increase the Fe abundance of the interstellar medium, thus accounting for the α -enhancement seen in the largest galaxies. The feedback from supernovae and from the active nucleus also determines the relationship between the black-hole mass and the mass, or the velocity dispersion, of the host galaxy, as well as the black-hole mass function. In both cases the model predictions are in excellent agreement with the observational data. Coupling the model with GRASIL (Silva et al. 1998), the code computing in a self-consistent way the chemical and spectrophotometric evolution of galaxies over a very wide wavelength interval, we have obtained predictions in excellent agreement with observations for a number of observables which proved to be extremely challenging for all the current semi-analytic models, including the sub-mm counts and the corresponding redshift distributions, and the epoch-dependent K-band luminosity function of spheroidal galaxies.

Subject headings: galaxies: elliptical and lenticular, lCD — galaxies: evolution — galaxies: formation — QSOs: formation

1. Introduction

Although the traditional approach to galaxy formation and evolution regards nuclear activity as an incidental diversion, it is becoming clear, beyond any reasonable doubt, that the formation of super-massive black holes powering nuclear activity is intimately linked to the formation of its host galaxy and plays a key role in shaping its evolution. Evidences supporting this view include: the discovery that Massive Dark Objects (MDOs), with masses in the range $\sim 10^6$ – $3 \times 10^9 M_\odot$ and a mass function matching that of baryons accreted onto black holes during the quasar activity (Salucci et al. 1999), are present in essentially all local galaxies with a substantial spheroidal component (Kormendy & Richstone 1995; Magorrian et al. 1998; van der Marel 1999; Kormendy & Gebhardt 2001); the tight correlation between the MDO mass (M_{BH}) and the velocity dispersion of stars in the host galaxy (Magorrian et al. 1998; Ferrarese & Merritt 2000; Gebhardt et al. 2000; Tremaine et al. 2002), the mass of the spheroidal component (McLure & Dunlop 2002; Dunlop et al. 2003; Marconi & Hunt 2003), and the mass of the dark halo (Ferrarese 2002); the correspondence between the luminosity function of active star-forming galaxies at $z \simeq 3$, the B-band luminosity function of quasars and the mass function of dark halos at the same redshift (Haehnelt et al. 1998, Monaco et al. 2000); the similarity between the evolutionary histories of the luminosity densities of galaxies and quasars (e.g. Cavaliere & Vittorini 1998). Recently Shields et al. (2003) have found that the correlation between M_{BH} and the stellar velocity dispersion is already present at redshift up to ~ 3 .

As discussed by Granato et al. (2001), the mutual feedback between galaxies and quasars during their early evolutionary stages may be the key to overcome some of the crises of the currently standard scenario for galaxy evolution. For example, predictions of semi-analytic models (Devriendt & Guiderdoni 2000; Cole et al. 2000; Somerville et

al. 2001; Menci et al. 2002) are persistently unable to account for the surface density of massive galaxies at substantial redshift detected by (sub)-mm surveys with SCUBA and MAMBO (Blain et al. 2002; Scott et al. 2002) and by deep K-band surveys (Cimatti et al. 2002b; Kashikawa et al. 2003), unless ad-hoc adjustments are introduced. The difficulty stems from the fact that the standard CDM scenario tends to imply that most of the star formation occurs in relatively small galaxies that later merge to make bigger and bigger objects. On the contrary, the data indicate that galaxies detected by (sub)-mm surveys are mostly very massive, with very high star-formation rates ($\sim 10^3 M_\odot \text{yr}^{-1}$), at $z > 2$ (Dunlop 2001; Ivison et al. 2002; Aretxaga et al. 2003; Chapman et al. 2003). All these data are more consistent with the traditional “monolithic” scenario, according to which elliptical galaxies formed most of their stars in a single burst, at relatively high redshifts, and underwent essentially passive evolution thereafter. On the other hand, the “monolithic” scheme is inadequate to the extent that it cannot be fitted in a consistent scenario for structure formation from primordial density perturbations.

Clues on the timing of evolution of both galaxies and quasars are provided by chemical abundances (e.g. Friaça & Terlevich 1998). Spectroscopic observations demonstrate, even for the highest redshift quasars, a fast metal enrichment of the circum-nuclear gas (e.g. Hamann & Ferland 1999; Fan et al. 2000, 2001; Freudling et al. 2003). Statistical studies of local E/S0 galaxies, hosting super-massive black-holes, show that the most massive galaxies are also the most metal rich, the reddest, and, perhaps, the oldest (Forbes & Ponman 1999; Trager et al. 2000a,b). Such galaxies show an excess α -elements/ Fe ratio, compared to solar (α -enhancement; Trager et al. 2000a,b; Thomas et al. 2002), suggestive of very intense but short star-formation activity. Also observations of hosts of high redshift quasars show that they are as massive as expected from the local L_{QSO} - L_{host} relation, and that most of their stars are relatively old, although star forming regions are present (Kukula et al. 2001; Hutchings et al. 2002; Ridgway et al. 2002; Stockton & Ridgway 2001).

The work carried out by our group in the last several years, aimed at constructing physically

¹INAF - Osservatorio Astronomico di Padova, Vicolo Osservatorio, I-35100 Padova, Italy

²International School for Advanced Studies, SISSA/ISAS, Via Beirut 2-4, I-34014 Trieste, Italy

³INAF - Osservatorio Astronomico di Trieste, Via G.B. Tiepolo 11, I-34131 Trieste, Italy

grounded models for the joint formation and evolution of quasars and spheroidal galaxies in the framework of the standard hierarchical clustering scenario (Granato et al. 2001), has shown that, to account for the surface density of massive galaxies at substantial redshifts detected by sub-mm SCUBA surveys (which turns out to be far in excess of predictions of standard semi-analytic models), allowing for the observed relationships between quasars and galaxies, it is necessary to assume that the formation of stars and of the central black hole took place on shorter timescales within more massive dark matter halos. In other words, the canonical hierarchical CDM scheme - small clumps collapse first - is reversed for baryon collapse and the formation of luminous objects (*Anti-hierarchical Baryon Collapse* scenario). This behavior, attributed to the feedback from supernova explosions and, for the most massive galaxies, from nuclear activity, may account simultaneously for evolutionary properties of quasars and of massive spheroidal galaxies (Monaco et al. 2000; Granato et al. 2001), for clustering properties of SCUBA galaxies (Magliocchetti et al. 2002; Perrotta et al. 2003), and for the metal abundances in spheroidal galaxies and in bulges of later Hubble types hosting super-massive black holes (Romano et al. 2002).

Recently, Cattaneo & Bernardi (2003), using the early type galaxy sample in the Sloan Digital Sky Survey (Bernardi et al. 2003a), investigated the hypothesis that quasars formed together with the stellar population of ellipticals, finding a consistency with the observed luminosity function of optical quasars.

However, there is not, as yet, a clear understanding of the physical mechanisms governing the interactions among the active nucleus and the host galaxy. Silk & Rees (1998) and Fabian (1999) proposed that the relationship between the black-hole mass and the velocity dispersion (or mass) of the host stellar spheroid may be the effect of the quasar feedback. However, in its present form, the proposed mechanism does not imply shorter star-formation times for more massive galaxies and therefore cannot easily explain the α -enhancement of more massive objects. Wang & Biermann (1998) suggested that the formation of both elliptical galaxies and super-massive black-holes at their centers is related to the merging of two proto-

disks. Kauffmann & Haehnelt (2000) and Haehnelt & Kauffmann (2000) have analyzed the evolution of active nuclei and of host galaxies in the framework of the hierarchical clustering scenario, using a semi-analytic approach. In their scheme, the merging process determines both the evolution of galaxies and the growth of the black-holes at their centers. This model predicts a rapid evolution of galaxies with redshift. Volonteri et al. (2002, 2003) presented a model in which most of the mass in BHs is assembled in accretion episodes triggered by merging. They found that the galaxy merging would leave about 10% of massive black-holes distributed in galactic halos and a similar fraction of binary super-massive black-holes in galactic centers. Di Matteo et al. (2003) considered the gas content in galaxies, as predicted by cosmological hydrodynamical simulations including sub-grid prescriptions for gas cooling and star formation (but not for BH growth). They pointed out that the observed $M_{\text{BH}}-\sigma$ correlation is well reproduced, provided that a linear relationship between the gas and BH masses (at $z > 1$) is assumed.

In this paper we carry out an investigation of the physical processes driving the growth of the central black hole and the effect of the energy released by the active nucleus on the surrounding proto-galactic gas. The corresponding prescriptions for matter outflow, gas cooling and collapse, star formation, etc. are implemented in a model for the formation and evolution of galaxies, interfaced with our code computing their spectral energy distribution as a function of their age, taking into account the evolution of stellar populations, of metal abundances, of the dust content and its distribution (GRASIL: Silva et al. 1998, Silva 1999, Granato et al. 2000). Our aim is to put on a more solid physical basis the approach by Granato et al. (2001), which partly relies on empirical recipes.

The model has been tested against the observed correlation of BH masses with the mass and velocity dispersion of the host galaxies, the observed K-band and sub-millimeter counts and the associated redshift distributions, along with the chemical and photometric properties of the local E/S0 galaxies. In subsequent papers the model will be used to predict the time-dependent luminosity function of quasars up to $z > 6$ and of passively evolving ellipticals, and their clustering properties, with ref-

erence to the observational capabilities of space missions such as SIRTF, to be launched in a few months, JWST, of ground millimeter telescopes such as ALMA, and of the forthcoming deep near-IR surveys from the ground.

In Sect. 2 we describe the basic physical processes governing the evolution of the star-formation rate in spheroidal galaxies, the growth of central black-holes and their feedback. In Sect. 3 we present our main results, which are discussed in Sect. 4. In Sect. 5 we summarize our main conclusions.

We adopt a cold dark matter cosmology with cosmological constant, consistent with the Wilkinson Microwave Anisotropy Probe (WMAP) data (Bennett et al. 2003), as well as with information from large scale structure (Spergel et al. 2003): $\Omega_m = 0.29$, $\Omega_b = 0.047$, and $\Omega_\Lambda = 0.71$, $H_0 = 72 \text{ km s}^{-1}$, $\sigma_8 = 0.8$, and an index $n = 1.0$ for the power spectrum of primordial density fluctuations.

2. Basic ingredients

2.1. Dark matter halos

Following Navarro et al. (1997) and Bullock et al. (2001b) we identify as a virialized halo at redshift z a volume of the Universe of radius r_{vir} enclosing an overdensity $\Delta_{\text{vir}}(z)$ which, for a flat cosmology, can be approximated by

$$\Delta_{\text{vir}} \simeq \frac{(18\pi^2 + 82x - 39x^2)}{\Omega(z)}, \quad (1)$$

where $x = \Omega(z) - 1$ and $\Omega(z)$ is the ratio of the mean matter density to the critical density at redshift z (Bryan & Norman 1998). The halo mass is then given by

$$M_{\text{vir}} = \frac{4\pi}{3} \Delta_{\text{vir}}(z) \rho_u(z) r_{\text{vir}}^3, \quad (2)$$

$\rho_u(z)$ being the mean universal matter density. Useful quantities are the rotational velocity of the DM halo at its virial radius, $V_{\text{vir}}^2 = GM_{\text{vir}}/r_{\text{vir}}$, and the equilibrium gas temperature in the DM potential well

$$kT = \frac{1}{2} \mu m_p V_{\text{vir}}^2, \quad (3)$$

where m_p is the proton mass and μm_p is the mean molecular weight of the gas.

The virialized halos exhibit a universal density profile (Navarro et al. 1997; Bullock et al. 2001b) well described by

$$\rho(r) = \frac{\rho_s}{c x (1 + c x)^2}, \quad (4)$$

where $x = r/r_{\text{vir}}$ and c is the concentration parameter. Analyzing the profiles of a large sample of virialized halos obtained through high-resolution N-body simulations, Bullock et al. (2001b) found that, at any redshift, c is a weak function of the mass $c \propto M_{\text{vir}}^{-0.13}$, while, at fixed mass, $c \propto (1+z)^{-1}$.

Numerical simulations and theoretical arguments show that the dark matter assembly in halos proceeds through a first phase of fast accretion, followed by a slow phase (Wechsler et al. 2002; van den Bosch 2002). Zhao et al. (2003) showed that the potential well of the halos is built up during the fast accretion. The subsequent slow accretion does not change the “identity” of the halo, though significantly increasing its mass. Guided by these results, in the following we will assume that, for the mass and redshift ranges we are interested in, the virialization epoch of DM halos coincides with the end of the fast accretion phase and with the beginning of the vigorous star formation of the proto-spheroidal galaxies, and that these galaxies keep their identity till the present time. Our approach implies, in the mass and redshift range considered, a one to one correspondence between halos and galaxies, consistent with the available data on clustering of Lyman-break (Bullock et al. 2002) and SCUBA galaxies (Magliocchetti et al. 2001; Perrotta et al. 2003).

The formation rate of massive halos ($M_{\text{vir}} \gtrsim 2.5 \times 10^{11} M_\odot$) at $z \gtrsim 1.5$ is approximated by the positive part of the time derivative of the halo mass function $n(M_{\text{vir}}, z)$ (Haehnelt & Rees 1993; Sasaki 1994; Peacock 1999). The negative part is small for this mass and redshift range, consistent with our assumption that massive halos survive till the present time. Following Press & Schechter (1974) we write:

$$n(M_{\text{vir}}, z) = \frac{\rho}{M_{\text{vir}}^2} \nu f(\nu) \frac{d \ln \nu}{d \ln M_{\text{vir}}} \quad (5)$$

where ρ is the average comoving density of the universe and $\nu = [\delta_c(z)/\sigma_\delta(M_{\text{vir}})]^2$, σ_δ being the rms initial density fluctuations smoothed on a scale

containing a mass M_{vir} , and δ_c the critical over-density for spherical collapse. The latter quantity is given by $\delta_c(z) = \delta_0/b(z)$, δ_0 being the present day critical over-density (1.686 for an Einstein–de Sitter cosmology, with only negligible dependencies on Ω_m and Ω_Λ) and $b(z)$ the linear growth factor, for which we adopt the approximation proposed by Li & Ostriker (2002). For the function $\nu f(\nu)$ we adopt the expression given by Sheth & Tormen (2002), which also takes into account the effect of ellipsoidal collapse:

$$\nu f(\nu) = A[1 + (a\nu)^{-p}](\frac{a\nu}{2})^{1/2} \frac{e^{-a\nu/2}}{\pi^{1/2}}, \quad (6)$$

where $A = 0.322$, $p = 0.3$ and $a = 0.707$.

2.2. Star-formation rate

Recent studies on the angular momentum of dark matter (DM) halos suggest that a significant fraction of the mass has a low specific angular momentum (Bullock et al. 2001a). Also, the results of high resolution simulations including gas suggest that a significant fraction of the angular momentum of the baryons is redistributed to the dark matter by dynamical friction (see e.g. Navarro & Steinmetz 2000), although the heating of the gas in sub-galactic halos may increase the tidal stripping and the angular momentum of the gas (Maller & Dekel 2002). As far as the effect of angular momentum can be neglected, as is probably the case for the formation of spheroidal galaxies, the collapse time of baryons within the host dark matter halo, t_{coll} , is the maximum between the free-fall time,

$$t_{\text{dyn}}(r) = [3\pi/32G\rho(r)]^{1/2}, \quad (7)$$

and the cooling time

$$t_{\text{cool}}(r) = \frac{3}{2} \frac{\rho_{\text{gas}}(r)}{\mu m_p} \frac{kT}{C n_e^2(r) \Lambda(T)}, \quad (8)$$

both computed at the virial time t_{vir} . In the above equations ρ is the total matter density, ρ_{gas} is the gas density, n_e is the electron density, $\Lambda(T)$ is the cooling function and $C = \langle n_e^2(r) \rangle / \langle n_e(r) \rangle^2$ is the clumping factor, assumed constant. In the following we adopt the cooling function given by Sutherland & Dopita (1993), which includes the dependence on metal abundance.

We consider a single-zone galaxy with three gas phases: diffuse gas in the outer regions, with

mass $M_{\text{inf}}(t)$, infalling on a dynamical timescale, cool gas with mass $M_{\text{cold}}(t)$, available to form stars, and hot gas with mass $M_{\text{hot}}(t)$, eventually outflowing. At the virialization we assume that $M_{\text{inf}}(t_{\text{vir}}) = f_b M_{\text{vir}}$, with $f_b = 0.16$, the universal ratio of baryons to DM (Bennett et al. 2003; Spergel et al. 2003). The infalling gas, initially at the equilibrium temperature in the DM potential well [Eq. (3)], is transferred to the cool star-forming phase at a rate:

$$\dot{M}_{\text{cold}}(t) = M_{\text{inf}}(t) / \max[t_{\text{cool}}(r_{\text{vir}}), t_{\text{dyn}}(r_{\text{vir}})]. \quad (9)$$

The star formation rate (SFR) is given by:

$$\psi(t) = \int_0^{r_{\text{vir}}} \frac{1}{\max[t_{\text{cool}}(r), t_{\text{dyn}}(r)]} \frac{dM_{\text{cold}}(r, t)}{dr} dr, \quad (10)$$

where we assume that the cold gas distribution still follows the DM distribution. This assumption is admittedly quite unrealistic since cold cloudlets should rather fall towards the center. But again, a realistic modelling of the cold gas distribution would be too ambitious at the present stage.

As mentioned above, according to recent studies (Wechsler et al. 2002, van den Bosch 2002, Zhao et al. 2003) while the build-up of the potential well is rather fast, the mass of the halo goes on increasing over a time scale of the order of the Hubble time. The baryons associated with this slow accretion occupy a large volume so that have a relatively low density and feel also the heating effect of the supernova and quasar feedback. It is therefore reasonable to assume that their cooling time is comparable to, or longer than, the Hubble time, and does not partake in the star formation process.

Strictly speaking, in Eq. (9) the increase of the cooling time due to the dilution of the hot gas as the cold gas drops out should be taken into account. The effect is, however, minor because the fraction of gas in the cold phase is always $< 50\%$ and can therefore be ignored given the exploratory nature of the present model.

Although the Initial Mass Function (IMF) may depend on the physical properties of the gas, such as density and metallicity (see Eisenhauer 2001 and references therein), it is often assumed to be independent of time and galaxy mass. We will consider in the following the IMF preferred by Romano et al (2002) on the basis of chemi-

cal abundances in local ellipticals, i.e. $\Phi(M) \propto M^{-0.4}$ for $M \leq 1 M_\odot$ and $\Phi(M) \propto M^{-1.25}$ for $1 M_\odot < M \leq 100 M_\odot$. A detailed discussion of the effects of varying the IMF on the properties of the present day elliptical galaxies will be presented in a forthcoming paper.

The feedback due to supernova (SN) explosions moves the gas from the cold to the hot phase at a rate:

$$\dot{M}_{\text{cold}}^{\text{SN}} = -\frac{2}{3}\psi(t)\epsilon_{\text{SN}}\frac{\eta_{\text{SN}}E_{\text{SN}}}{\sigma^2}, \quad (11)$$

where η_{SN} is the number of Type II SNe expected per solar mass of formed stars (determined by the IMF, adopting a minimum progenitor mass of $8 M_\odot$), E_{SN} is the kinetic energy of the ejecta from each supernova (10^{51} erg; e.g. Woosley & Weaver 1986), and ϵ_{SN} is the fraction of this energy which is used to reheat the cold gas. Analyses show that about 90% of the SN kinetic energy may be lost by radiative cooling (Thornton et al. 1998; Heckman et al. 2000); we adopt $\epsilon_{\text{SN}} = 0.05$ as our reference value, consistent with the results by Mac Low & Ferrara (1999) and Wada & Venkatesan (2003).

We relate V_{vir} to the line-of-sight velocity dispersion σ using the relationship $\sigma/V_{\text{vir}} \simeq 0.65$, derived by Ferrarese (2002) for a sample of local galaxies.

The chemical evolution of the gas is followed by using classical equations and stellar nucleosynthesis prescriptions, as for instance reported in Romano et al. (2002).

We can elucidate the dependence of the star formation rate on halo mass by means of a simple order of magnitude argument. Since the mean density within the virial radius is $\simeq 200\rho_{\text{crit}}$, the mean value of t_{dyn} is about a factor of 10 shorter than the expansion timescale, at all redshifts, independently of the halo mass. If the gas is in virial equilibrium in the DM potential well, the effective cooling time of a pure hydrogen plasma is, assuming uniform density:

$$t_{\text{cool,eff}} \simeq 1.6 \cdot 10^{11} (1 + z_{\text{vir}})^{-5/2} h^{1/3} \cdot \left(\frac{M_{\text{vir}}}{10^{12} M_\odot}\right)^{1/3} \left(\frac{M_{\text{vir}}/M_{\text{gas}}}{1/0.16}\right)^{1/2} C^{-1} \text{ yr} \quad (12)$$

As discussed by Romano et al. (2002, cf. their Fig. 10), for spheroidal galaxies with $\lesssim 10^{11} M_\odot$ in stars, the ratio between M_{vir} and the mass in stars at $z=0$ (including remnants) M_{sph} decreases

with increasing M_{sph} , roughly as:

$$M_{\text{vir}}/M_{\text{sph}} \propto M_{\text{sph}}^{-1/3}, \quad (13)$$

due to the larger effect of stellar feedback in shallower potential wells. Since the mass of cooling gas is approximately equal to M_{sph} , $t_{\text{cool,eff}}$ turns out to be very weakly dependent on M_{vir} . For an effective clumping factor $C_{\text{eff}} \gtrsim 10$, Eq. (12), yields a cooling time shorter than the mean free-fall time for $z \gtrsim 3$, for all galactic masses. Allowing for the gas metallicity obviously decreases t_{cool} .

If the final mass in stars, M_{sph} , is proportional to the mass of the cooling gas, M_{sph} , Eq. (13) implies that, for galaxies with $M_{\text{sph}} < 10^{11} M_\odot$, $M_{\text{vir}} \propto M_{\text{sph}}^{2/3} \propto M_{\text{gas}}^{2/3}$. Thus the star formation rate, $\psi(t) \simeq M_{\text{gas}}/\max(t_{\text{cool}}, t_{\text{dyn}})$ is approximately $\propto M_{\text{vir}}^{3/2}$, since both timescales are effectively independent of, or very weakly dependent on, M_{vir} . This means that stars form faster within larger dark-matter halos, as in the *Anti-hierarchical Baryon Collapse* scenario by Granato et al. (2001). If, as argued above, the star formation rate is controlled by t_{dyn} , we have $\psi(t) \simeq 32(M_{\text{gas}}/10^{11} M_\odot)(1+z)^{3/2} M_\odot \text{ yr}^{-1}$.

2.3. Black-hole growth

As discussed by Haiman et al. (2003), the available information on the evolution of both the global star formation rate and the quasar emissivity is broadly consistent with the hypothesis that star formation in spheroids and black-hole (BH) fuelling are proportional to one another.

One mechanism yielding such proportionality has been discussed by Umemura (2001), Kawakatu & Umemura (2002) and Kawakatu et al. (2003). In the central regions of proto-galaxies the drag due to stellar radiation may result in a loss of angular momentum of the gas at a rate that in a clumpy medium is well approximated by

$$\frac{d \ln J}{dt} \simeq \frac{L_{\text{sph}}}{c^2 M_{\text{gas}}} (1 - e^{-\tau}), \quad (14)$$

where L_{sph} is the global stellar luminosity and τ is the effective optical depth of the spheroid. The latter quantity is given by $\tau = \bar{\tau} N_{\text{int}}$, where $\bar{\tau}$ is the average optical depth of single clouds and N_{int} is the average number of clouds intersected by a light ray over a typical galactic path.

The gas can then flow towards the center, feeding a mass reservoir around the BH at a rate (Kawakatu et al. 2003)

$$\dot{M}_{\text{inflow}} \simeq -M_{\text{gas}} \frac{d \ln J}{dt} \simeq \left(\frac{L_{\text{sph}}}{c^2} \right) (1 - e^{-\tau}). \quad (15)$$

During the early evolutionary stages the luminosity is dominated by massive main sequence stars, $M \geq 5M_{\odot}$, and is thus proportional to the star formation rate $\psi(t)$. For the adopted IMF we have:

$$\dot{M}_{\text{inflow}} \simeq 1.2 \times 10^{-3} \psi(t) (1 - e^{-\tau}) M_{\odot} \text{ yr}^{-1}. \quad (16)$$

While this expression is useful for the analytical estimates presented in Sect. 3.1, in the full calculations we have adopted the values L_{sph} computed using our spectrophotometric code GRASIL. We parameterize the optical depth τ as:

$$\tau = \tau_0 \left(\frac{Z}{Z_{\odot}} \right) \left(\frac{M_{\text{gas}}}{10^{12} M_{\odot}} \right)^{\frac{1}{3}}, \quad (17)$$

and for τ_0 we explore the range from 1 to 10 (see Sect. 3).

An order of magnitude estimate of the relevant timescales and luminosities can be derived assuming that \dot{M}_{inflow} is directly the accretion rate on the central BH. Then, the timescale for it to grow to a mass M_{BH} is, using the order of magnitude estimate of $\psi(t)$ given in the previous section,

$$t_{\text{BH}} \simeq \frac{M_{\text{BH}}}{\dot{M}_{\text{inflow}}} \simeq 2.3 \times 10^9 \frac{M_{\text{BH}}}{10^8 M_{\odot}} \left(\frac{M_{\text{gas}}}{10^{11} M_{\odot}} \right)^{-1} \cdot (1+z)^{-3/2} (1 - e^{-\tau})^{-1} \text{ yr}. \quad (18)$$

Thus, if the accretion is not limited e.g. by radiation pressure or by angular momentum, black-holes can grow to very large masses from small (e.g., stellar mass) seeds in a time shorter than the age of the universe at all relevant redshifts. If $M_{\text{BH}} \propto M_{\text{gas}}$, the growth time is independent of M_{BH} .

For accretion with radiative efficiency η , the bolometric luminosity is $L_{\text{bol}} \simeq \eta \dot{M}_{\text{inflow}} c^2$. Following Elvis, Risaliti, & Zamorani (2002), we adopt, as a reference value, $\eta = 0.15$. In units of the Eddington luminosity

$$L_{\text{Edd}} \simeq 1.26 \times 10^{46} (M_{\text{BH}}(t)/10^8 M_{\odot}) \text{ erg s}^{-1}, \quad (19)$$

and setting $M_{\text{BH}}(t) \simeq \dot{M}_{\text{inflow}} t$, we have:

$$\frac{L_{\text{bol}}}{L_{\text{Edd}}} \simeq 3 \frac{\eta}{0.15} \left(\frac{t}{10^8 \text{ yr}} \right)^{-1}, \quad (20)$$

showing that the fast accretion phase and the build up of super-massive BH can be quite fast, thus accounting for QSO at high z .

Obviously, super-Eddington accretion is not the only mechanisms for a rapid black-hole growth. At the other extreme we may have accretion with low radiative efficiency such as the black-hole mergers at high redshifts advocated by Haiman et al. (2003), which may be testable by gravitational wave experiments like LISA (Menou, Haiman & Narayan 2001). Since these early evolutionary phases are expected to be heavily dust obscured, a powerful tool to discriminate among the various possibilities is hard X-ray emission. Far-IR/mm observations are also useful, but less capable of distinguishing the effect of the AGN from that of a starburst.

While mechanisms for super-Eddington accretion have been proposed (Begelman 2001, 2002), fully unperturbed free-fall is unrealistic. Correspondingly, $L_{\text{bol}}/L_{\text{Edd}}$ will not reach the extreme values indicated by Eq. (20) and the duration of the $L_{\text{bol}}/L_{\text{Edd}} \gtrsim 1$ phase can be longer. In our model, we first let the material infalling at the rate given by Eq. (15) accumulate in a circumnuclear mass reservoir, and then flow toward the black hole on a time scale depending on the viscous drag $\tau_{\text{visc}} \sim r^2/\nu$. The reservoir accumulates mass at a net rate $\dot{M}_{\text{res}} = \dot{M}_{\text{inflow}} - \dot{M}_{\text{BH}}$, where \dot{M}_{BH} is computed as follows. Following Duschl et al. (2000) and Burkert & Silk (2001) we adopt a viscosity $\nu = \mathcal{R}_{\text{crit}}^{-1} v_r$, where $\mathcal{R}_{\text{crit}} = 100\text{--}1000$ is the critical Reynolds number for the onset of turbulence. With these assumptions the viscous time can be expressed as $\tau_{\text{visc}} = \tau_{\text{dyn}} \mathcal{R}_{\text{crit}}$. The dynamical time $\tau_{\text{dyn}} = (3\pi/32G\rho_s)^{1/2}$ is referred to the system ‘black hole plus reservoir’.

The accretion radius of the BH is given by $r_a = GM_{\text{BH}}/V_{\text{vir}}^2$. Defining the reservoir dimension $R_{\text{res}} = \alpha r_a$, we estimate ρ_s as the mean density within a sphere of radius R_{res} with mass $M_{\text{BH}} + M_{\text{res}}$, to get:

$$\tau_{\text{dyn}} = \pi \left(\frac{\alpha}{2} \right)^{3/2} \frac{G}{V_{\text{vir}}^3} \frac{M_{\text{BH}}^{3/2}}{(M_{\text{BH}} + M_{\text{res}})^{1/2}}. \quad (21)$$

The viscous accretion rate onto the BH can be defined as

$$\dot{M}_{\text{BH}}^{\text{visc}} = \frac{M_{\text{res}}}{\tau_{\text{visc}}} = k_{\text{accr}} \frac{\sigma^3}{G} \left(\frac{M_{\text{res}}}{M_{\text{BH}}} \right)^{3/2} \left(1 + \frac{M_{\text{BH}}}{M_{\text{res}}} \right)^{1/2}. \quad (22)$$

The constant $k_{\text{accr}} = [\pi(\alpha/2)^{3/2}(V_{\text{vir}}/\sigma)^3\mathcal{R}_{\text{crit}}]^{-1}$ has a rather wide range of possible values. For $\mathcal{R}_{\text{crit}} = 100$ and $\alpha = 10$ we have $k_{\text{accr}} \sim 10^{-4}$ that we adopt as the reference value in the following. The actual accretion rate is then given by

$$\dot{M}_{\text{BH}} = \min(\dot{M}_{\text{BH}}^{\text{visc}}, \mathcal{A}M_{\text{Edd}}) \quad (23)$$

where $M_{\text{Edd}} = L_{\text{Edd}}/(\eta c^2)$ and $\mathcal{A} = (L/L_{\text{Edd}})_{\text{max}}$ is the maximum allowed Eddington ratio. In our computations, we allow at most mildly super-Eddington accretion, i.e. $\mathcal{A} \leq$ a few.

2.4. QSO feedback

The QSO activity affects the interstellar medium of the host galaxy and also the surrounding intergalactic medium through both the radiative output and the injection of kinetic energy producing powerful gas outflows. Quasar-driven outflows have been invoked to produce an intergalactic magnetic field (Furlanetto & Loeb 2001), and to preheat the intra-cluster medium (Valageas & Silk 1999; Kravtsov & Yepes 2000; Wu et al. 2000; Bower et al. 2001; Cavaliere et al. 2002; Platania et al. 2002). In the case of radio loud QSOs there is evidence that up to about half of the total power is in the jets (Rawlings & Saunders 1991; Celotti et al. 1997; Tavecchio et al. 2000). In broad absorption line (BAL) QSOs, the kinetic power of the outflowing gas can be a significant fraction of the bolometric luminosity (Begelman 2003). X-ray observations of BAL QSOs revealed significant absorption ($N_{\text{H}} \gtrsim 10^{23} \text{ cm}^{-2}$), implying large outflows ($\dot{M}_{\text{out}} \gtrsim 5 M_{\odot}/\text{yr}$) and large kinetic luminosities L_K (Brandt et al. 2001; Brandt & Gallagher 2000).

Theoretical studies on the mechanisms responsible for AGN-driven outflows show that efficient acceleration could be due to radiation pressure through scattering and absorption by dust (see e.g. Voit et al. 1993) and scattering in resonance lines (see e.g. Arav, Li & Begelman 1994). Murray et al. (1995) presented a dynamical model for a wind produced just over the disk by a combination of radiation and gas pressure. In a similar way Proga,

Stone & Kallman (2000) showed that a wind can be launched from a disc around a $10^8 M_{\odot}$ black hole with velocities up to $0.1c$ and mass-loss rate of $0.5 M_{\odot} \text{ yr}^{-1}$. Following Murray et al. (1995), an approximate solution for the wind velocity produced by line acceleration as a function of the radius is:

$$v = v_{\infty} \left(1 - \frac{r_f}{r} \right)^{2.35} \quad (24)$$

where r_f is the radius at which the wind is launched.

The asymptotic speed is

$$v_{\infty} \sim \left(\gamma \frac{GM_{\text{BH}}}{r_f} \right)^{1/2} \quad (25)$$

where γ is related to the force multiplier (see e.g. Laor & Brandt 2002). Adopting the reference values of the parameters of Murray et al. (1995), we have $\gamma \simeq 3.5$. By replacing the BH mass with the corresponding Eddington luminosity $L_{\text{Edd},46}$ in units of $10^{46} \text{ erg s}^{-1}$, we get:

$$\frac{v_{\infty}}{c} \sim 6.2 \times 10^{-2} \left(\frac{r_f}{10^{16} \text{ cm}} \right)^{-1/2} L_{\text{Edd},46}^{1/2}. \quad (26)$$

Detection of outflows with velocities ranging between $0.1c$ and $0.4c$ in the Broad Absorption Line (BAL) quasars APM08279 + 0522 (Chartas et al. 2002) and PG1115 + 080 (Chartas et al. 2003) has been reported, based on observations of X-ray broad absorption lines performed with the Chandra and XMM-Newton X-ray observatories. In the case of APM08279 + 0522 an intrinsic bolometric luminosity of $L_{\text{bol}} \sim 2.4 \times 10^{47} \text{ erg s}^{-1}$ has been estimated by Egami et al. (2000). Under the assumption of $L_{\text{Edd}} \sim 1-3 L_{\text{bol}}$, the maximum observed velocity $v \simeq 0.4c$ is obtained with a launching radius $r_f \sim 0.5-2 \times 10^{16} \text{ cm}$. Such small values of r_f are confirmed by the observed variability of the absorption line energies and widths in APM08279 + 0522 over a proper timescale of 1.8 weeks (Chartas et al. 2003).

The asymptotic speed is reached at $r \gtrsim 40r_f$. If f_c is the covering factor of the outflow and using $\dot{M}_w = 4\pi r^2 \rho(r) v_r \sim 4\pi f_c m_H N_H 40r_f v_{\infty}$, we get

$$\dot{M}_w = 2.6 f_c N_{22} L_{\text{Edd},46}^{1/2} \left(\frac{r_f}{10^{16} \text{ cm}} \right)^{1/2} M_{\odot} \text{ yr}^{-1} \quad (27)$$

where and $N_{22} = N_H/10^{22} \text{ cm}^{-2}$. Adopting $r_f = 1.5 \times 10^{16} \text{ cm}$ as a reference value, the kinetic power

in the outflow is

$$L_K = \frac{1}{2} \dot{M}_w v_\infty^2 \simeq 3.6 \times 10^{44} f_c N_{22} L_{\text{Edd},46}^{3/2} \text{ erg s}^{-1}, \quad (28)$$

and may thus amount to several percent of the accretion luminosity for highly luminous QSOs. Interestingly, this corresponds to the power required to account for the pre-heating of the intra-cluster medium (Bower et al. 2001; Platania et al. 2002; Lapi et al. 2003). It is also interesting to notice that $\dot{M}_w/\dot{M}_{\text{acc}} \simeq 2.5(\epsilon/0.1)f_c N_{22} L_{\text{Edd},46}^{-1/2}$, implying that for highly luminous QSOs $\dot{M}_w \sim \dot{M}_{\text{acc}}$, if $f_c N_{22} \sim 1$. High luminosity QSOs emitting at the Eddington limit are able to generate winds involving relatively small amounts of gas, but with very high velocities and significant kinetic energies. When the luminosity decreases below the Eddington limit we replace the Eddington luminosity with the bolometric luminosity in Eqs. (28) and (30).

Estimating the fraction of the kinetic luminosity L_K transferred to the interstellar medium is a rather complex problem. One possible effect of outflows and jets is to transport the ambient gas to larger radii. This effect has been recently estimated through numerical simulations by Brüggén et al. (2002). By investigating the effects of radio cocoons on the intra-cluster medium, they concluded that frequent low-power activity cycles are rather efficient in stirring the environment gas, particularly in regions close to the injection point of the high speed gas. Enßlin & Kaiser (2000) evaluated the energy accumulated in the cocoons around radio-galaxies. Inoue & Sasaki (2001) argued that for non relativistic cocoon plasma, the fraction of the jet energy deposited in the intra-cluster medium can reach 40%, neglecting the radiative cooling. Similar conclusions have been reached by Bicknell et al. (1997). Nath & Roychowdhury (2002), taking into account also the radiative losses, found that a large fraction ($\gtrsim 0.5$) of the kinetic energy of BAL and radio loud QSOs is transferred to an ambient gas with number density $n \simeq 0.1\text{--}1 \text{ cm}^{-3}$ and temperature $T_{\text{vir}} \simeq 10^6$ K. These values of density and temperature are quite similar to those of the gas in the outer regions of massive galactic halos.

We assume that the QSO feedback heats up the interstellar medium at a rate $L_h = f_h L_K$ and

removes it from the cold phase at a rate

$$\dot{M}_{\text{cold}}^{\text{QSO}} = -\frac{2}{3} \frac{L_h}{\sigma^2} \frac{M_{\text{cold}}}{M_{\text{gas}}}, \quad (29)$$

where $M_{\text{gas}} = M_{\text{cold}} + M_{\text{inf}}$ is the mass of the gas in the cold phase plus that of the gas which has not yet fallen in the star forming region. Setting $\epsilon_{\text{QSO}} = (f_h/0.5)(f_c/0.1)(N_{22}/10)$, we get

$$\dot{M}_{\text{cold}}^{\text{QSO}} \simeq -2 \times 10^3 \frac{\epsilon_{\text{QSO}} L_{\text{Edd},46}^{3/2}}{(\sigma/300 \text{ km s}^{-1})^2} \frac{M_{\text{cold}}}{M_{\text{gas}}} M_\odot \text{ yr}^{-1}, \quad (30)$$

We have explored the range $1 \leq \epsilon_{\text{QSO}} \leq 10$, adopting $\epsilon_{\text{QSO}} = 6$ as our reference value. The fraction $M_{\text{cold}}/M_{\text{gas}}$ in the right-hand side of Eq. (29) has been introduced in order to share the QSO feedback between the cold and the infalling gas. Thus the QSO feedback also removes the infalling gas at a rate

$$\dot{M}_{\text{inf}}^{\text{QSO}} = -\frac{2}{3} \frac{L_h}{\sigma^2} \frac{M_{\text{inf}}}{M_{\text{gas}}}. \quad (31)$$

The quasar feedback can easily heat the interstellar gas to temperatures $\sim 1 \text{ keV}$ (Valageas & Silk 1999; Bower et al. 2001; Nath & Roychowdhury 2002; Platania et al. 2002; Lapi et al. 2003), thus unbinding it and making it flow into the intergalactic medium (IGM). The corresponding energy injection in the IGM may account for the steepening of the X-ray luminosity–temperature correlation observed in groups of galaxies (O’Sullivan, Ponman, & Collins 2003). Given the low IGM gas density, only a small fraction of it will eventually cool down and fall back again to form stars.

Table 1: Model parameters, reference value and number of the equation where it is introduced (or short description).

Symbol	Value	Eq.
C	20	8
ϵ_{SN}	0.05	11
τ_0	4	17
k_{accr}	1×10^{-4}	22
M_{BHseed}	$10^3 M_\odot$	Seed BH mass
$(L/L_{\text{Edd}})_{\text{max}}$	3	23
ϵ_{QSO}	6.0	30
η	0.15	20

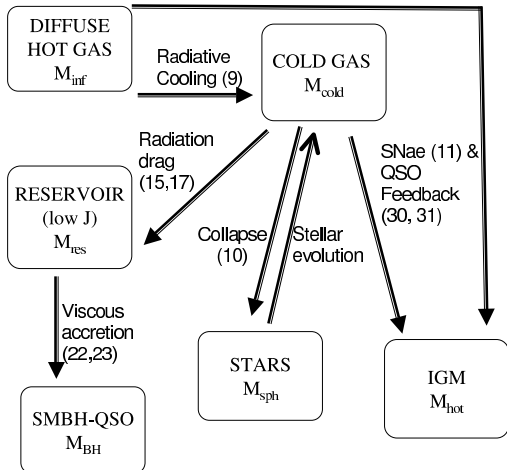


Fig. 1.— Scheme of the baryonic components included in the model (boxes), and of the corresponding mass transfer processes (arrows). The numbers near the arrows point to the main equations describing those processes.

3. Results

The results presented here refer to halos with mass in the range $2.5 \times 10^{11} M_{\odot} \lesssim M_{\text{vir}} \lesssim 1.6 \times 10^{13} M_{\odot}$, formed at $z_{\text{vir}} \gtrsim 1.5$. This lower limit to the virialization redshift allows us to crudely filter out halos hosting discs and irregular galaxies. In our view, late-virialized objects had more time to acquire a substantial angular momentum and are less likely to take on an early-type morphology. This is in keeping with the common notion that stellar populations in disks are on average substantially younger than those in spheroids.

The model, whose main baryonic components and corresponding mass transfer are sketched in Fig. 1, allows us to follow the star formation and chemical enrichment histories of spheroidal galaxies, as well as the growth of their central BHs, once the virialization time and the halo mass is given. Interfacing it with the code GRASIL (see Silva et al. 1998 for details), which computes the spectrophotometric evolution from radio to X-ray wavelengths including the dust effects, we get the spectral properties of the spheroidal galaxies as a function of cosmic time. In the application of GRASIL, we have made the standard assumption that the starburst is highly obscured throughout

its duration, with an $1 \mu\text{m}$ optical depth of molecular clouds, where new stars are born, of $\tau_1 = 30$ for solar metallicity, and scaling linearly with Z . As for the dust emissivity index, we have adopted the canonical value of 2. The results presented in this paper are only weakly sensitive to variations of τ_1 by a factor of several.

The relationship between τ_1 and the optical depth given by Eq. (17) is not straightforward. The starlight is processed by dust within molecular clouds and re-emitted in the far-IR, with a peak at $60\text{--}100 \mu\text{m}$. At these wavelengths, the optical depth is lower than that at $1 \mu\text{m}$ by a factor $\sim 10^{-2}$. The effective optical depth to the inter-cloud radiation, responsible for the drag exerted on gas clouds as discussed in Sect. 2.3, is therefore $\tau \sim 10^{-2} \tau_1 N_{\text{int}}$, where N_{int} is the mean number of clouds intersected by a photon (Kawakatu & Umemura 2002). The latter number depends, among other things, on the radial distribution of the clouds within the galaxy. For instance, a population of giant molecular clouds with a typical size of 10 pc , masses of the order of $10^5 M_{\odot}$, uniformly distributed in the central $\sim 10 \text{ kpc}$ of the galaxy, give $N_{\text{int}} \sim 10$, for $M_{\text{gas}} \simeq 10^{12} M_{\odot}$. As anticipated, for τ_0 [Eq. (17)] we explored the range 1–10.

In this Section we present some of the most important results, obtained using the reference values of the parameters already discussed and summarized in Table 1. The discussion of the effects of varying the parameters within the allowed ranges will be presented in the next Section.

Examples of the time evolution of the various components for different virialization redshifts and halo masses are shown in Fig. 2 and Fig. 3.

3.1. Time delay between star formation and QSO activity

A key result of the model is the prediction of the time delay between the onset of vigorous star formation, at the virialization epoch, and the peak of the QSO activity. The combined action of stellar and nuclear feedbacks, eventually sweeping out the interstellar medium, determines the duration of the star formation.

As shown in Fig. 4 the duration of the most active star formation phase decreases with increasing M_{vir} and z_{vir} . The timescale T_{100} is defined as the

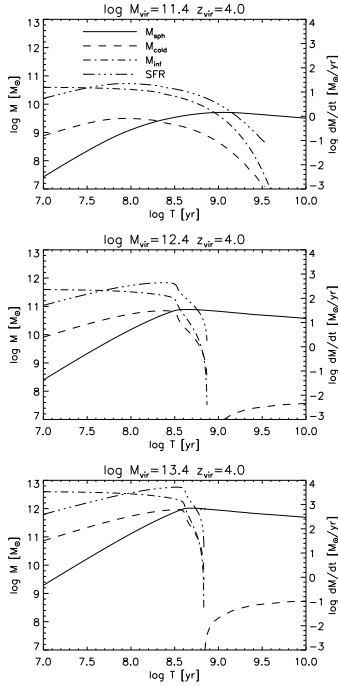


Fig. 2.— Evolution of the mass in stars, in the cold (M_{cold}) and infalling (M_{inf}) gas components, and of the Star Formation Rate, as a function of the galactic age T , for 3 values of M_{vir} and $z_{\text{vir}} = 4$. Note the sharp break corresponding to the sweeping out of the interstellar medium by the quasar feedback, for large M_{vir} .

galactic age at which the gas mass still available for star formation or accretion, i.e. $M_{\text{cool}} + M_{\text{inf}}$, is reduced to 1% of the initial value. This corresponds approximately to the duration of the star formation burst empirically estimated by Granato et al. (2001), and given by their Eq. (8). In the redshift range $3 \lesssim z_{\text{vir}} \lesssim 6$, $T_{100} \simeq 0.5\text{--}1$ Gyr for $M_{\text{vir}} \gtrsim 10^{12} M_{\odot}$, corresponding (see Fig. 5) to $M_{\text{sph}} \gtrsim 2.5 \times 10^{10} M_{\odot}$. For smaller masses the duration of the actively star forming phase increases to reach 1.5-3 Gyr for $M_{\text{sph}} \simeq 3 \times 10^9 M_{\odot}$, if virialized at $z_{\text{vir}} \gtrsim 3$, and is even longer if virialization occurs at lower z .

A feeling of the role of the main ingredients of the model in shaping this result can be obtained ignoring the reservoir, so that the inflow onto the central black hole is governed by Eq. (15). The inflow is definitively halted at a time t_{out} when the energy injected by the QSO in the interstellar

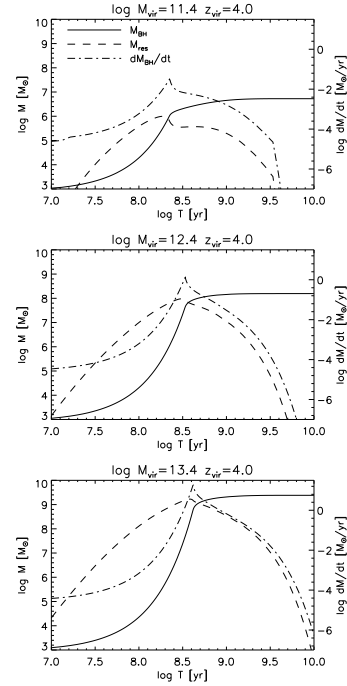


Fig. 3.— Growth of the black-hole and of the reservoir as a function of the galactic age T , for the same values of M_{vir} and $z_{\text{vir}} = 4$ as in Fig. 2. The apex of dM_{BH}/dt corresponds to the end of the exponential growth of the black-hole mass, when the mass accretion rate becomes insufficient to support the adopted maximum Eddington ratio, $(L/L_{\text{Edd}})_{\text{max}} = 3$.

medium equals the binding energy of the gas (cf. Cavaliere et al. 2002):

$$\int_0^{t_{\text{out}}} f_h L_K dt = M_{\text{vir}} V_{\text{vir}}^2, \quad (32)$$

where V_{vir} is related to the mass inside the virial radius, M_{vir} , by (Bullock et al. 2001b):

$$V_{\text{vir}} = 75(1 + z_{\text{vir}})^{1/2} \left(\frac{M_{\text{vir}}}{10^{11} h^{-1} M_{\odot}} \right)^{1/3} \text{ km s}^{-1}. \quad (33)$$

Using Eq. (28) and Eq. (18) with $\exp(-\tau) \ll 1$, and assuming that the black hole growth occurs in a time shorter than the expansion timescale, we obtain:

$$t_{\text{out}} \simeq 7.9 \times 10^8 h^{4/15} f_h^{-2/5} (1 + z_{\text{vir}})^{-1/2} \cdot \left(\frac{M_{\text{vir}}}{10^{12} M_{\odot}} \right)^{2/3} \left(\frac{M_{\text{gas}}}{10^{11} M_{\odot}} \right)^{-3/5}$$

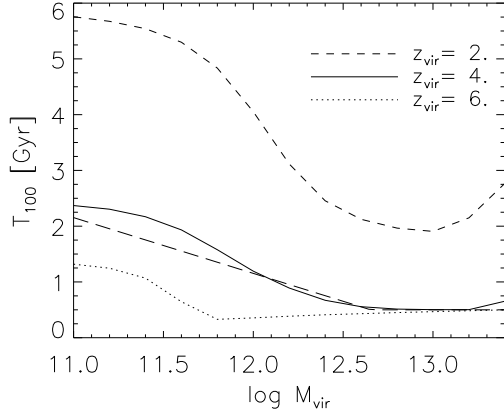


Fig. 4.— Duration of the star-formation burst as a function of M_{vir} , for 3 values of z_{vir} (see text for the exact definition of T_{100}). For our choice of the parameters, at low z_{vir} the cooling time becomes longer than the dynamical time at large masses, causing the upturn of T_{100} . The long-dashed line close to the solid line corresponding to $z_{\text{vir}} = 4$ represents the empirical recipe adopted by Granato et al. (2001).

$$\begin{aligned} &\simeq 1.2 \times 10^9 h^{4/15} f_h^{-2/5} \cdot \\ &\cdot (1 + z_{\text{vir}})^{-1/2} \left(\frac{M_{\text{vir}}}{10^{12} M_{\odot}} \right)^{-7/30} \text{yr} \end{aligned} \quad (34)$$

where the last step follows from Eq. (13), normalized to $M_{\text{vir}}/M_{\text{sph}} \simeq 20$ for $M_{\text{sph}} = 5 \times 10^{10} M_{\odot}$, assuming $M_{\text{gas}} \simeq M_{\text{sph}}$.

The final black-hole mass (except for the effect of later re-activation phases) can be roughly estimated to be $\sim M_{\text{BH}}(t_{\text{out}})$:

$$\begin{aligned} M_{\text{BH}}(t_{\text{out}}) &\simeq 4.3 \times 10^7 h^{4/15} f_h^{-2/5} \cdot \\ &\cdot \left(\frac{M_{\text{vir}}}{10^{12} M_{\odot}} \right)^{2/3} \left(\frac{M_{\text{gas}}}{10^{11} M_{\odot}} \right)^{2/5} (1 + z_{\text{vir}}) M_{\odot} \\ &\simeq 3.2 \times 10^7 h^{4/15} f_h^{-2/5} \cdot \\ &\cdot \left(\frac{M_{\text{vir}}}{10^{12} M_{\odot}} \right)^{19/15} (1 + z_{\text{vir}}) M_{\odot} \\ &\simeq 2.5 \times 10^8 \left(\frac{h}{0.7} \right)^{-1} \left(\frac{f_h}{0.3} \right)^{-2/5} \cdot \\ &\cdot \left(\frac{\sigma}{200 \text{km/s}} \right)^{19/5} \left(\frac{1 + z_{\text{vir}}}{4} \right)^{-9/10} M_{\odot} \end{aligned} \quad (35)$$

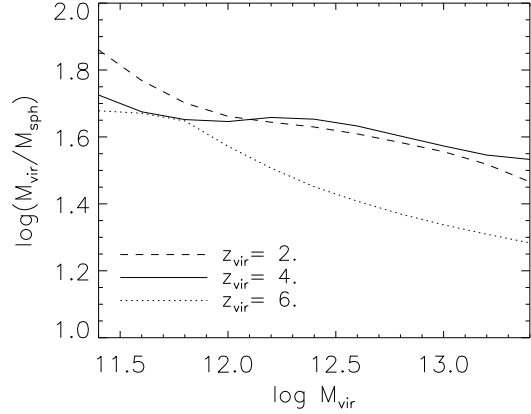


Fig. 5.— Virial to stellar mass ratio at the present time as a function of M_{vir} for 3 values of z_{vir} .

where we have used Eqs. (13) and (33), and have adopted the relationship $\sigma \simeq 0.65 V_{\text{vir}}$ (Ferrarese 2002). This result is in remarkably good agreement with the determination by Gebhardt et al. (2000) of the $M_{\text{BH}}-\sigma$ relationship. A full comparison of our model predictions with observational data is shown in Fig. 6, where the expected spread due to the distribution of virialization redshifts is also illustrated. Note the predicted fall-off of M_{BH} at low values of σ , due to the combined effect of SN feedback which is increasingly efficient with decreasing halo mass in slowing down the gas infall onto the central BH, and of the decreased radiation drag due to a decrease of τ [Eq. (17)], which is, for these objects, $\ll 1$. This steepening of the lower part of the $M_{\text{BH}}-\sigma$ relationship translates in a *flattening* of the lower part of the $M_{\text{vir}}-M_{\text{BH}}$ correlation, in agreement with the results reported in Fig. 5 of Ferrarese (2002).

In Fig. 7 the predicted BH mass function at $z = 0$ is shown against the local BH mass function recently derived by Shankar et al. (in preparation) following Salucci et al. (1999). The total local BH mass density is estimated to be $5.2 \times 10^5 M_{\odot} \text{Mpc}^{-3}$.

The physics that rules the fast growth of the central BH in massive halos is the key point: its growth is paralleled by an increasing feedback from the nuclear activity. In the most massive halos the quasar feedback eventually removes most of the gas (and dust), leaving the nucleus shining

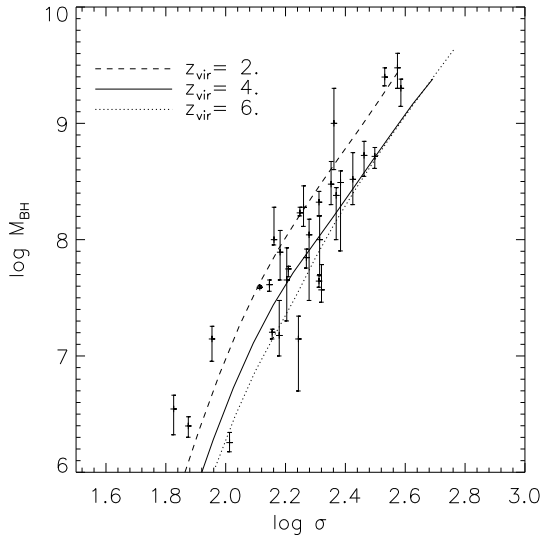


Fig. 6.— Predicted relationship between black-hole mass and line-of-sight velocity dispersion of the host galaxy for different virialization redshifts. Data are from Tremaine et al. (2002).

as an optical quasar until the reservoir mass is exhausted on a timescale $\sim 10^7$ yr (see Fig. 3). Since then the host galaxy evolves passively and the BH becomes dormant (apart from possible reactivations). The process slows down with decreasing halo mass, as the supernova feedback becomes increasingly important.

3.2. Photometric properties and metal abundances of spheroidal galaxies

In small halos ($M_{\text{vir}} \lesssim 10^{11} M_{\odot}$) the star formation rate is kept low by stellar feedback, which heats up most of the gas and moves it to lower density outskirts, where the cooling time is very long. Only when the virial mass exceeds a few $10^{11} M_{\odot}$ the potential wells are deep enough to allow a more effective star formation. Figure 5 shows the dependence on M_{vir} of the ratio $M_{\text{vir}}/M_{\text{sph}}$, for three values of z_{vir} . Bright galaxies virializing at $z \lesssim 4$ are predicted to have $M_{\text{vir}}/M_{\text{sph}} \simeq 40$. For comparison, McKay et al. (2002) report, for bright galaxies, M/L values in the SDSS g -band of 171 ± 40 based on the dynamics of satellites, and of 270 ± 35 based on weak lensing measurements; adopting for the stellar component of early-type

galaxies $M/L_V \simeq 4\text{--}5.9$ (Fukugita et al. 1998) this translates (for $L_V \simeq L_g$) into $M_{\text{vir}}/M_{\text{sph}} \simeq 30\text{--}70$.

Once the star formation law is specified, the chemical evolution of the galaxy is followed by using classical equations and stellar nucleosynthesis prescriptions (Granato et al. 2001). The predicted mean metallicity, $\langle Z_{\star} \rangle$ in stars is shown, as a function of the mass in stars, in Fig. 8. The average metallicity increases from about half solar to super-solar with increasing galaxy mass. In particular, for our reference model, the metal content is super-solar for $M_{\text{vir}} \gtrsim 5 \times 10^{11} M_{\odot}$, or $M_{\text{sph}} \gtrsim 10^{10} M_{\odot}$.

It should be stressed that this result refers to the average metallicity of the galaxies, since our model is one-zone. In the central regions, star-formation, and consequently metal enrichment, is faster because of the higher densities entailing shorter dynamical times. Adopting densities appropriate for the innermost 10% of the galaxy mass, the predicted metallicity of the gas is between 3 to 5 times solar, with a general trend at increasing with M_{vir} . This result compares fairly well with several recent **direct** chemical measurements of circum-nuclear gas in high- z QSO (e.g. Dietrich et al. 2003).

Another evident trend is the increase with the galaxy mass of the ratio between the abundance of the so-called α -elements and that of Fe . Fig. 9 shows the mean $[Mg/Fe]$ ratio, in stars, as a function of the galaxy mass for three different values of the virialization redshift. The ratio $[Mg/Fe]$ is always super-solar, and is further enhanced for $M_{\text{vir}} \gtrsim 10^{12} M_{\odot}$. However, in spite of the high metallicity reached by our models, we find that the average stellar $[Fe/H]$ is always subsolar (≤ -0.25). This trend is dictated by the mass dependence of T_{100} : in high mass objects the star-formation activity is essentially ended when SNIa start to pollute the ISM with Fe .

Both the trend of the global metallicity and the ratio of the α -elements to Fe abundance with the galaxy mass, are in fair agreement with what is inferred from the spectrophotometric observations of local early type galaxies. The narrowness and the inclination of the color-magnitude relation of elliptical galaxies hints at a rapid formation process and at a range in metallicity from about half solar to twice solar (e.g. Bressan, Chiosi & Fagotto 1994). Furthermore, narrow band obser-

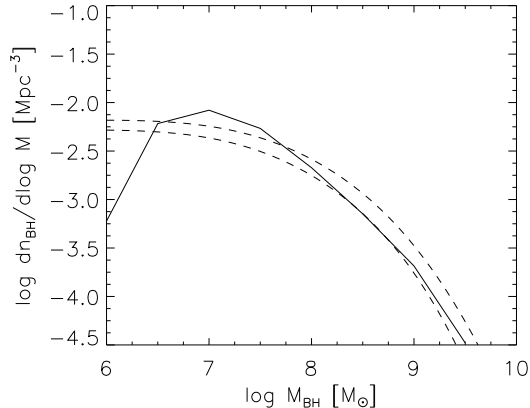


Fig. 7.— Predicted local black-hole mass function (solid line) compared with the recent estimate by Shankar et al. (in preparation, region delimited by the two thin dashed lines). The total mass density in BHs they derive is $\rho_{BH} \simeq 4 \times 10^5 M_\odot \text{Mpc}^{-3}$, 25% less than our model. The decline of the model at low M_{BH} is due to having considered only objects with $M_{vir} \geq 2.5 \times 10^{11} M_\odot$.

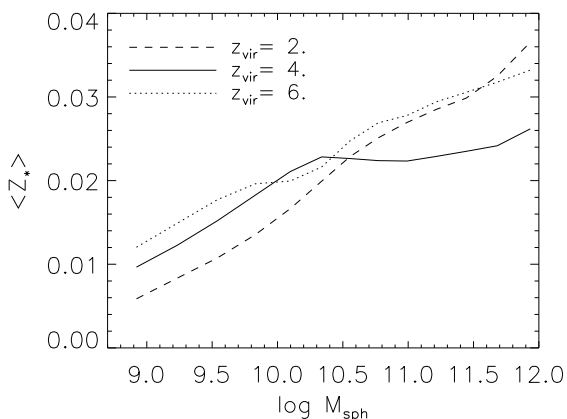


Fig. 8.— Mean stellar metallicity as a function of the present-day stellar mass for the usual 3 values of z_{vir} .

vations not only provide evidence for a similar spread in metallicity (Bernardi et al. 2003b), but also demand a significant enhancement of the α -elements in the more massive ellipticals (Worthey et al. 1994). The observed run of Mg and Fe narrow band indices with the luminosity of the galaxy or with the $H\beta$ index, cannot be reproduced by stellar population models based solely on solar partition of heavy elements (Worthey et al. 1994; Trager et al. 2000a,b; Bernardi et al. 2003b).

It is worth noticing at this level that while the model reproduces, for a relatively broad range of parameter choices, the main trends of the metal abundances inferred from observations of local ellipticals, our predictions cannot yet be directly compared with observations. For example, narrow band indices show a complicated dependence on global metallicity, partition of heavy elements and age of the stellar populations, that render the adoption of common scaling relations (e.g. Matteucci, Ponzzone & Gibson 1998) quite uncertain. We should thus generate mock catalogues of local early type galaxies and investigate their spectrophotometric properties by means of adequate spectral synthesis tools. Work in this direction is in progress and will be reported in a subsequent paper.

3.3. Luminosity function of early-type galaxies

In these galaxies the K-band luminosity is a quite good indicator of the mass in stars. In Fig. 10 we compare the modelled K-band local luminosity function with the recent determinations by Kochanek et al. (2001) and Huang et al. (2003). As already remarked, the solid line includes the contribution of all spheroids with mass in the range $2.5 \times 10^{11} \lesssim M_{vir} \lesssim 1.6 \times 10^{13}$, formed at $z_{vir} \gtrsim 1.5$. According to our model, spheroidal galaxies born in halos with $M_{vir} \lesssim 2.5 \times 10^{11} M_\odot$ have masses in stars $M_{sph} \lesssim 10^9 M_\odot$ and K-band magnitudes $\gtrsim -21.3$ (cfr. Fig. 5).

For a more direct comparison with the observational data, the dot-dashed line in Fig. 10 shows the predicted local luminosity function for early-type galaxies only. It was obtained subtracting from the results shown by the solid line, the contributions of bulges of Sa and Sb galaxies estimated using the local B-band luminosity functions and

the bulge-to-total luminosity ratios for galaxies of these morphological types derived by Salucci et al. (1999) and adopting a color $B-K = 4.1$. It should also be noted that the mass in stars for small halos is strongly dependent on the stellar feedback, namely on the IMF and on the SN efficiency ϵ_{SN} : an increase of the efficiency from 0.1 to 0.3 results in a decrease of mass in stars by a factor $\simeq 3$. This dependence weakens with increasing M_{vir} .

Figure 11 compares the predicted rest-frame K-band luminosity function at $z = 1.5$ with the observational determination by Pozzetti et al. (2003), which, at the highest luminosities, is substantially above predictions of the models by Kauffmann et al. (1999), Cole et al. (2000), and Menci et al. (2002).

3.4. SCUBA galaxies and EROs

In large galactic halos the star formation rate turns out to be very high at high redshift, yielding a quick increase of the metallicity and of the dust mass. The latter is computed by GRASIL as proportional to the product of the gas mass by its metallicity, with a coefficient determined by the condition of a gas-to-dust ratio of 110 for solar metallicity (Silva et al. 1998). Thus, most of the star formation occurs in a dusty environment, so that these galaxies are powerful far-IR/sub-mm sources, highly obscured in the visual and near IR bands. In Fig. 12 we have plotted the model predictions at $850 \mu\text{m}$ against the SCUBA counts. The predicted redshift distributions are similar to those shown by Granato et al. (2001). In particular, for a flux density limit of 5 mJy, the model gives a median redshift of 2.2 and an inter-quartile range of 1.6–3.3, to be compared with $z_{\text{median}} = 2.4$ and the inter-quartile range of 1.9–2.8 found for the sample of Chapman et al. (2003).

After the interstellar medium has been swept out, galaxies evolve passively. The combination of redshift and aging soon makes them extremely red. We computed the expected contribution to the extragalactic K-band counts of spheroidal galaxies in this phase. A comparison (Fig. 13) of the predicted with the observed redshift distribution of galaxies with $K \leq 20$ (Cimatti et al. 2002b) shows that they fully saturate the high redshift tail of the distribution.

Cimatti et al. (2002a) selected a complete sample of Extremely Red Objects (EROs) ($(R-K_s) \geq 5$) with $K < 19.2$. More than 60% of the objects have redshift, mostly spectroscopic. On the basis of the spectra, the sample has been subdivided into dusty and non-dusty EROs. Their data suggest that there is a significant number of *old* dust-free ellipticals in place at $z \geq 1$. This result is confirmed by the subsequent analysis by Pozzetti et al. (2003), who found that the bright end of the K-band luminosity function at $z \geq 1$ is dominated by red/early type galaxies. Our model is consistent with these results (cf. Fig. 11).

Our expectation of the existence of a significant population of luminous red galaxies at substantial redshifts is also borne out by the results of the very deep near-infrared photometry of the Hubble Deep Field-South with ISAAC on the VLT (Franx et al. 2003) and by follow-up Keck spectroscopy (van Dokkum et al. 2003). Model predictions closely match the surface density ($3 \pm 0.8 \text{ arcmin}^{-2}$) and the median redshift (2.6) of galaxies with $K_s < 22.5$ and $(J_s - K_s) > 2.3$ (Franx et al. 2003).

4. Discussion

To highlight the dependence of galaxy properties on their halo masses, we make reference to three characteristic values, namely $M_{\text{vir}} \simeq 10^{11.4}$, $10^{12.4}$ and $10^{13.4}$, referred to as low, intermediate and high masses, respectively.

The clumping factor C affects only the evolution of high and intermediate masses, where a decrease of C from 20 to 1 strongly inhibits the capability of gas to quickly cool down, form stars and feed the BH. For large galactic masses, the star-formation activity and the growth of the BH, rather than being confined to the first ~ 1 Gyr after virialization, continues for a time comparable to the Hubble time. However, the final ratio $M_{\text{BH}}/M_{\text{sph}}$ is almost the same, both masses ultimately depending on the SFR. Conversely, at lower masses the collapse becomes increasingly limited by the dynamical time even when $C = 1$.

The supernova efficiency ϵ_{SN} has some effect on the evolution at all masses: $M_{\text{sph}}, \langle Z_* \rangle$ and $M_{\text{BH}}/M_{\text{sph}}$ decrease with increasing ϵ_{SN} , while T_{100} increases. Differences are modest at high masses, but become dramatic at low masses. At $M_{\text{vir}} \lesssim 2 \times 10^{11} M_{\odot}$ and $\epsilon_{\text{SN}} \gtrsim 0.2$, the evolu-

tion of the star-formation rate can show damped oscillations at early epochs ($T \lesssim 1$ Gyr).

By converse, the QSO efficiency, ϵ_{QSO} , influences only intermediate and large masses, where an increase of this parameter determines a shorter active star forming phase, and lower values of $\langle Z_* \rangle$, M_{sph} and M_{QSO} , while the ratio $M_{\text{BH}}/M_{\text{sph}}$ is little affected. An increase of the radiative efficiency ϵ has a very similar effect.

When the accretion is Eddington-limited (or, at most, mildly super-Eddington), T_{100} , $\langle Z_* \rangle$, and M_{sph} decrease with increasing seed BH mass: less e-folding times are necessary to produce substantial effects on the environment. Typically, M_{sph} decreases by 30% when the seed mass is increased from 10^3 to $10^4 M_{\odot}$, but the ratio $M_{\text{BH}}/M_{\text{sph}}$ decreases by less than 10%. As already remarked, the development of low masses is instead weakly affected by the BH feedback. By converse, if substantially super-Eddington accretion is allowed, the model is quite insensitive to the precise choice of the seed BH mass.

The ratio between QSO and SN feedback is an increasing function of the virial mass of the galaxy (see Fig. 14). For low mass galaxies the integrated effect of the QSO is almost negligible compared to that of SNaE, but takes over (typically by a factor of a few) for intermediate masses ($M_{\text{vir}} \sim 10^{12.4} M_{\odot}$), and dominates (by a factor $\gtrsim 10$) at high masses ($M_{\text{vir}} \sim 10^{13.4} M_{\odot}$). Note that the QSO effect usually increases exponentially with time, while that of SNaE increases more slowly. Thus the instantaneous QSO effect becomes dominant, if ever, only a few e-folding times before the maximum of QSO activity.

As mentioned at the beginning of Sect. 3, our definition of a galactic halo associated with a spheroidal galaxy is rather crude. However, the successful comparison with the observed population properties of spheroidal galaxies (Figs. 7, 10, 11, 12, 13, and 15) gives us some confidence about the meaningfulness of the criterion we have adopted.

Although we have not addressed the details of the formation of disk (and irregular) galaxies, we envisage them as associated primarily to halos virializing at $z_{\text{vir}} \lesssim 1.5$, which have incorporated, through merging processes, a large fraction of halos less massive than $2.5 \times 10^{11} M_{\odot}$ virializing at

earlier times. These low mass halos virialized at early times may become the bulges of late type galaxies.

5. Summary and conclusions

We have presented a detailed, physically grounded, model for the early co-evolution of spheroidal galaxies and of active nuclei at their centers. The model is based on very simple recipes, that can be easily implemented. In summary, we start from the diffuse gas within the dark matter halo falling down into the star forming regions at a rate ruled by the dynamic and the cooling times. Part of this gas condenses into stars, at a rate again controlled by the local dynamic and cooling times. But the gas also feels the feedback from supernovae and from active nuclei, heating it and possibly expelling it from the potential well. Also the radiation drag on the cold gas decreases its angular momentum, causing an inflow into a reservoir around the central black hole. Viscous drag then causes the gas to flow from the reservoir into the black hole, increasing its mass and powering the nuclear activity.

In the shallower potential wells (corresponding to lower halo masses and, for given mass, to lower virialization redshifts), the supernova heating is increasingly effective in slowing down the star formation and in driving gas outflows, resulting in an increase of star/dark-matter ratio with increasing halo mass. As a consequence, the star formation is faster within the most massive halos, and the more so if they virialize at substantial redshifts. Thus, in keeping with the proposition by Granato et al. (2001), physical processes acting on baryons effectively reverse the order of formation of galaxies compared to that of dark-matter halos.

A higher star-formation rate also implies a higher radiation drag, resulting in a faster loss of angular momentum of the gas (Umemura 2001; Kawakatu & Umemura 2002; Kawakatu et al. 2003) and, consequently, in a faster inflow towards the central black-hole. In turn, the kinetic energy carried by outflows driven by active nuclei through line acceleration is proportional to $M_{\text{BH}}^{3/2}$ (Murray et al. 1995), and this mechanism can inject in the interstellar medium a sufficient amount of energy to unbind it. The time required to sweep out the interstellar medium, thus halting both the star for-

mation and the black-hole growth, is again shorter for larger halos. For the most massive galaxies ($M_{\text{vir}} \gtrsim 10^{12} M_{\odot}$) virializing at $3 \lesssim z_{\text{vir}} \lesssim 6$, this time is < 1 Gyr, so that the bulk of the star-formation may be completed before type Ia supernovae can significantly increase the *Fe* abundance of the interstellar medium; this process can then account for the α -enhancement seen in the largest galaxies.

The interplay between star formation and nuclear activity determines the relationship between the black-hole mass and the mass, or velocity dispersion, of the host galaxy, as well as the black-hole mass function. As illustrated by Figs. 6 and 7, the model predictions are in excellent agreement with the observational data. A specific prediction of the model is a substantial steepening of the $M_{\text{BH}}-\sigma$ relation for $\sigma \lesssim 150 \text{ km s}^{-1}$: the mass of the BH associated to less massive halos is lower than expected from an extrapolation from higher masses, because of the combined effect of SN heating, which is increasingly effective with decreasing galaxy mass in hindering the gas inflow towards the central BH, and of the decreased radiation drag [see Eq. (15), with $\tau \ll 1$].

Coupling the model with GRASIL (Silva et al. 1998), the code computing in a self-consistent way the chemical and spectrophotometric evolution of galaxies over a very wide wavelength interval, we have obtained predictions for the sub-mm counts and the corresponding redshift distributions as well as for the redshift distributions of sources detected by deep K-band surveys, which proved to be extremely challenging for all the current semi-analytic models. The results, shown by Figs. 12 and 13, are again very encouraging.

A discussion of the evolutionary properties of AGNs predicted by the present model is deferred to a future paper, where we will address, among other things, the complex issue of how the bolometric luminosity produced by accretion processes shows up in different electromagnetic bands. We note however that the analysis by Granato et al. (2001), who approached the problem the other way round, i.e. inferred the formation history of spheroidal galaxies and of galactic bulges from the observed epoch-dependent luminosity function of quasars, got results in detailed agreement with those presented here. Thus an at least qualitative agreement of the present model with the data

on AGNs seems to be ensured. This is confirmed by the successful comparison of our model predictions for the relationship among the black-hole mass and the velocity dispersion of the host galaxy (Fig. 6), and for the local black-hole mass function (Fig. 7). Also, the predicted history of global accretion rate onto the central black-holes (Fig. 15), which, in our scheme, is directly proportional to the history of the bolometric luminosity density produced by AGNs, with its peak in the redshift range 2 to 3, is nicely consistent with the results of optical surveys (see, e.g., Fig. 8 of Fan et al. 2003).

Acknowledgments Work supported in part by MIUR and ASI. We warmly thank the referee for her/his constructive comments.

REFERENCES

- Arav, N., Li, Z., & Begelman, M.C. 1994, ApJ, 432, 62
- Aretxaga, I., Hughes, D.H., Chapin, E.L., Gaztanaga, E., Dunl J.S., & Ivison, R. 2003, MNRAS, in press
- Barger, A.J., Cowie, L.L., & Sanders, D.B. 1999, ApJ, 518, L5
- Begelman, M.C. 2001, ApJ, 551, 897
- Begelman, M.C. 2002, ApJ, 568, L97
- Begelman, M.C. 2003, in Carnegie Observatories Astrophysics Series, Vol. 1: Coevolution of Black Holes and Galaxies, ed. L.C. Ho (Cambridge: Cambridge Univ. Press), in press, astro-ph/0303040
- Bennett, C.L., et al. 2003, ApJ, 583, 1
- Bernardi, M., et al. 2003a, AJ, 125, 1817
- Bernardi, M., et al. 2003b, AJ, 125, 1882
- Bicknell, G.V., Dopita, M.A., & O’Dea, C.P.O. 1997, ApJ, 485, 112
- Blain, A.W., Kneib, J.-P., Ivison, R.J., & Smail, I. 1999, ApJ, 512, L87
- Blain, A.W., Smail, I., Ivison, R.J., Kneib, J.-P., & Frayer, D.T., 2002, PhR, 369, 111
- Borys, C., Chapman, S.C., Halpern, M., & Scott, D. 2002, MNRAS, 330, L63

- Bower, R.G., Benson, A.J., Lacey, C.G., Baugh, C.M., Cole, S., & Frenk, C.S. 2001, *MNRAS*, 325, 497
- Brandt, W.N., & Gallagher, S.C. 2000, *NewAR*, 44, 461
- Brandt, W.N., Gallagher, S.C., & Kaspi, S. 2001, in *New Century of X-ray Astronomy*, ed. H. Inoue & H. Kunieda (ASP Conf. Ser. 251; S. Francisco: ASP), 128
- Bressan, A., Chiosi, C., & Fagotto, F. 1994, *ApJS*, 94, 63
- Brüggen, M., Kaiser, C.R., Churazov, E., Enßlin, T.A. 2002, *MNRAS*, 331, 545
- Bullock, J.S., Dekel, A., Kolatt, T.S., Kravtsov, A.V., Klypin, A.A., Porciani, C., & Primack, J.R. 2001a, *ApJ*, 555, 240
- Bullock, J.S., Kolatt, T.S., Sigad, Y., Somerville, R.S., Kravtsov, A.V., Klypin, A.A., Primack, J.R., & Dekel, A. 2001b, *MNRAS*, 321, 559
- Bullock, J.S., Wechsler, R.H., & Somerville, R.S. 2002, *MNRAS*, 329, 246
- Burkert, A., & Silk, J. 2001, *ApJ*, 554, L151
- Cattaneo, A., & Bernardi, M., 2003, *MNRAS*, in press
- Cavaliere, A., Lapi, A., & Menci, N. 2002, *ApJ*, 581, L1
- Cavaliere, A., & Vittorini V. 1998, in *The Young Universe: Galaxy Formation and Evolution at Intermediate and High Redshift*, ed. S. D'Odorico, A. Fontana, & E. Giallongo (ASP Conf. Ser. 146; S. Francisco: ASP), 26
- Celotti, A., Padovani, P., & Ghisellini, G. 1997, *MNRAS*, 286, 415
- Chapman, S.C., Blain, A.W., Ivison, R.J., & Smail, I.R. 2003, *Nat*, 422, 695
- Chapman, S.C., Scott, D., Borys, C., & Fahlman, G.G. 2002, *MNRAS*, 330, 92
- Chartas, G., Brandt, W.N., & Gallagher, S.C. 2003, *ApJ* in press, astro-ph/0306125
- Chartas, G., Brandt, W.N., Gallagher, S.C., & Garmire, G.P. 2002, *ApJ*, 579, 169
- Cimatti, A., et al. 2002a, *A&A*, 381, L68
- Cimatti, A., et al. 2002b, *A&A*, 391, L1
- Cole, S., Lacey, C.G., Baugh, C.M., & Frenk, C.S. 2000, *MNRAS*, 319, 168
- Dietrich, M., Hamman, F., Schields, J.C., Constantin, A., Heidt, J., Jäger, K., Vestergaard, M., & Wagner, S.J. 2003, *ApJ*, 589, 722
- Devriendt, J.E.G., & Guiderdoni, B., 2000 *A&A*, 363, 851
- Di Matteo, T., Croft, R.A.C., Springel, V., & Hernquist, L., 2003, *ApJ*, 593, 56
- Dunlop, J.S. 2001, *NewAR*, 45, 609
- Dunlop, J.S., McLure, R.J., Kukula, M.J., Baum, S.A., O'Dea, C.P., Hughes, D.H. 2003, *MNRAS*, 340, 1095
- Duschl, W.J. Strittmatter, P.A., & Biermann, P.L. 2000, *A&A*, 357, 1123
- Eales, S., Lilly, S., Webb, T., Dunne, L., Gear, W., Clements, D., & Yun, M. 2000, *AJ*, 120, 2244
- Egami, E., Neugebauer, G., Soifer, B.T., Matthews, K., Ressler, M., Becklin, E.E., Murphy, T.W. Jr., & Dale, D.A. 2000, *ApJ*, 535, 561
- Eisenhauer, F. 2001, in *Science with the Large Binocular Telescope*, ed. T. Herbst, (Neumann Druck), 89
- Elvis, M., Risaliti, G., & Zamorani, G. 2002, *ApJ*, 565, L75
- Enßlin, T.A., & Kaiser, C.R. 2000, *A&A*, 360, 417
- Fabian, A.C. 1999, *MNRAS*, 308, L39
- Fan, X., et al. 2000, *AJ*, 120, 1167
- Fan, X., et al. 2001, *AJ*, 122, 2833
- Fan, X., et al. 2003, *AJ*, 125, 1649
- Ferrarese, L. 2002, *ApJ*, 578, 90
- Ferrarese, L., & Merritt, D. 2000, *ApJ*, 539, L9
- Forbes, D.A., & Ponman, T.J. 1999, *MNRAS*, 309, 623

- Franx, M., et al. 2003, ApJ, 587, L79
- Freudling, W., Corbin, M.R., & Korista, K.T. 2003, ApJ, 587, L67
- Friça, A.C.S., & Terlevich, R.J. 1998, MNRAS, 298, 399
- Furlanetto, S.R., & Loeb, A. 2001, ApJ, 556, 619
- Gebhardt, K., et al. 2000, ApJ, 539, L13
- Granato, G.L., Lacey, C.G., Silva, L., Bressan, A., Baugh, C.M., Cole, S., & Frenk, C.S. 2000, ApJ, 542, 710
- Granato, G.L., Silva, L., Monaco, P., Panuzzo, P., Salucci, P., De Zotti, G., & Danese, L. 2001, MNRAS, 324, 757
- Heckman, T.M., Lehnert, M.D., Strickland, D.K., & Armus, L. 2000, ApJS, 129, 493
- Haehnelt, M.G., & Kauffmann, G. 2000, MNRAS, 318, L35
- Haehnelt, M.G., Natarajan P. & Rees, M.J. 1998, MNRAS, 300, 817
- Haehnelt, M.G., & Rees, M.J. 1993, MNRAS, 263, 168
- Haiman, Z., Ciotti, L., & Ostriker, J.P., 2003, ApJ, submitt astro-ph/0304129
- Hamann, F., & Ferland, G. 1999, ARA&A, 37, 487
- Huang, J.-S., Glazebrook, K., Cowie, L.L., & Tinney, C. 2003, ApJ, 584, 203
- Hughes, D.H., et al. 1998, Nature, 394, 241
- Hutchings, J.B., Frenette, D., Hanisch, R., Mo, J., Dumont, P.J., Redding, D.C., & Neff, S.G. 2002, AJ, 123, 2936
- Inoue, S., & Sasaki, S. 2001, ApJ, 562, 618 2002, ApJ, 565, 63
- Iverson, R.J., et al. 2002, MNRAS, 337, 1
- Kashikawa, N., et al. 2003, AJ, 125, 53
- Kauffmann, G., Colberg, J.M., Diaferio, A., & White, S.D.M. 1999, MNRAS, 303, 188
- Kauffmann, G., & Haehnelt, M. 2000, MNRAS, 311, 576
- Kawakatu, N., & Umemura, M. 2002, MNRAS, 329, 572
- Kawakatu, N., Umemura, M., & Mori, M. 2003, ApJ, 583, 85
- Kochanek, C.S., et al. 2001, ApJ, 560, 566
- Kormendy, J., & Gebhardt, K., 2001, in 20th Texas Symposium on relativistic astrophysics, ed. J.C. Wheeler, & H. Martel (AIP Conf. Proc. 586; Melville: AIP), 363
- Kormendy, J., & Richstone, D. 1995, ARA&A, 33, 581
- Kravtsov, A.V., & Yepes, G. 2000, MNRAS, 318, 227
- Kukula M.J., Dunlop, J.S., McLure, R.J., Miller, L., Percival, W.J., Baum, S.A., & O'Dea, C.P. 2001, MNRAS, 326, 1533
- Laor, A., & Brandt, W.N. 2002, ApJ, 569, 641
- Lapi, A., Cavaliere, A., & De Zotti, G. 2003, ApJ, submitted
- Larson, R.B. 1998, MNRAS, 301, 569
- Li, L., & Ostriker, J.P. 2002, ApJ, 566, 652
- Mac Low, M., & Ferrara, A., 1999, ApJ, 513, 142
- Magliocchetti, M., Moscardini, L., Panuzzo, P., Granato, G.L., De Zotti, G., & Danese, L. 2001, MNRAS, 325, 1553
- Magorrian, J., et al. 1998, AJ, 115, 2285
- Maller, A.H., & Dekel, A. 2002, MNRAS, 335, 487
- Marconi, A., & Hunt, L. 2003, ApJL, 589, L21
- Matteucci, F., Ponzzone, R., & Gibson, B.K. 1998, A&A, 335, 855
- McLure, R.J., & Dunlop, J.S. 2002, MNRAS, 331, 795
- Menci, N., Cavaliere, A., Fontana, A., Giallongo, E., & Poli, F. 2002, ApJ, 575, 18
- Menou, K., Haiman, Z., & Narayan, V.K. 2001, ApJ, 558, 535

- Monaco, P., Salucci, P., & Danese, L. 2000, MNRAS, 311, 279
- Murray, N., Chiang, J., Grossman, S.A., & Voit, G.M. 1995, ApJ, 451, 498
- Nath, B.B., & Roychowdhury, S. 2002, MNRAS, 333, 145
- Navarro, J.F., Frenk, C.S., & White, S.D.M. 1997, ApJ, 490, 493
- Navarro, J.F., & Steinmetz, M. 2000, ApJ, 538, 477
- Peacock, J.A. 1999, *Cosmological Physics* (Cambridge, Cambridge University Press)
- O'Sullivan, E., Ponman, T.J., Collins, R.S. 2003, MNRAS, 340, 1375
- Perrotta, F., Magliocchetti, M., Baccigalupi, C., Bartelmann, M., De Zotti, G., Granato, G.L., Silva, L., & Danese, L. 2003, MNRAS, 338, 623
- Platania, P., Burigana, C., De Zotti, G., Lazzaro, E., & Bersanelli, M. 2002, MNRAS, 337, 242
- Pozzetti, L., et al. 2003, A&A, 402, 837
- Press, W.H., & Schechter, P. 1974, ApJ, 187, 425
- Proga, D., Stone, J.M., & Kallman, T.R. 2000, ApJ, 543, 686
- Ridgway, S. Heckman, T., Calzetti, D., & Lehnert, M. 2002, NewAR, 46, 175
- Romano, D., Silva, L., Matteucci, F., Danese, L. 2002, MNRAS, 334, 444
- Rawlings, S., & Saunders, R. 1991, Nat, 349, 138
- Salucci, P. Szuszkiewicz, E., Monaco, P., & Danese L. 1999, MNRAS, 307, 637
- Sasaki, S. 1994, PASJ, 46, 427
- Scott S.E., Fox, M.J., Dunlop, J.S., et al. 2002, MNRAS, 331, 817
- Sheth, R.K., et al. 2003, ApJ, submitted, astro-ph/0303092
- Sheth, R.K., & Tormen, G. 2002, MNRAS, 329, 61
- Shields, G.A., Gebhardt, K., Salviander, S., Wills, B.J., Xie, B., Brotherton, M.S., Yuan, J., & Dietrich, M. 2003, ApJ, 583, 124
- Silk, J., & Rees, M.J. 1998, A&A, 331, L1
- Silva, L. 1999, Ph.D. Thesis, SISSA, Trieste
- Silva, L., Granato, G.L., Bressan, A., & Danese, L. 1998, ApJ, 509, 103
- Somerville, R.S., Primack, J.R., & Faber, S.M. 2001, MNRAS, 320, 504
- Spergel, D.N., et al. 2003, ApJ, submitted, astro-ph/0302209
- Stockton, A., & Ridgway, S.E. 2001, ApJ, 554, 1012
- Sutherland, R.S., & Dopita, M.A. 1993, ApJS, 88, 253
- Tavecchio, F., et al. 2000, ApJ, 543, 535
- Thomas, D., Maraston, C., & Bender, R. 2002, Ap&SS, 281, 371
- Thornton, K., Gaudlitz, M., Janka, H.-T., & Steinmetz, M. 1998, ApJ, 500, 95
- Trager, S.C., Faber, S.M., Worthey, G., & González, J.J. 2000a, AJ, 119, 1645
- Trager, S.C., Faber, S.M., Worthey, G., & González, J.J. 2000b, AJ, 120, 165
- Tremaine, S., et al. 2002, ApJ, 574, 740
- Umemura, M. 2001, ApJ, 560, L29
- van Dokkum, P.G., et al. 2003, ApJ, 587, L83
- Valageas, P., & Silk, J. 1999, A&A, 350, 725
- van den Bosch, F.C., 2002, MNRAS, 331, 98
- van der Marel, R.P. 1999, AJ, 117, 744
- Voit, G.M., Weymann, R.J., & Korista, K.T. 1993, ApJ, 413, 95
- Volonteri, M., Haardt, F., & Madau, P. 2002, Ap&SS, 281, 501
- Volonteri, M., Haardt, F., & Madau, P. 2003, ApJ, 582, 559

Wang, Y., & Biermann, P.L. 1998, in Dynamics of Galaxies and Galactic Nuclei, ed. W.J. Duschl, & C. Einsel, 203

Wada, K., & Venkatesan, A. 2003, ApJ, 591, 38

Wechsler, R.H., Bullock, J.S., Primack, J.R., Kravtsov, A.V., & Dekel, A. 2002, ApJ, 568, 52

Wosley, S.E., & Weaver, T.A. 1986, ARA&A, 24, 205

Worthey, G., Faber, S.M., Gonzalez, J.J., & Burstein, D. 1994, ApJS, 94, 687

Wu, K.K.S., Fabian, A.C., & Nulsen, P.E.J. 2000, MNRAS, 318, 889

Zhao, D.H., Mo, H.J., Jing, Y.P., & Börner, G. 2003, MNRAS, 339, 12

Zepf, S.E., & Silk, J. 1996, ApJ, 466, 114

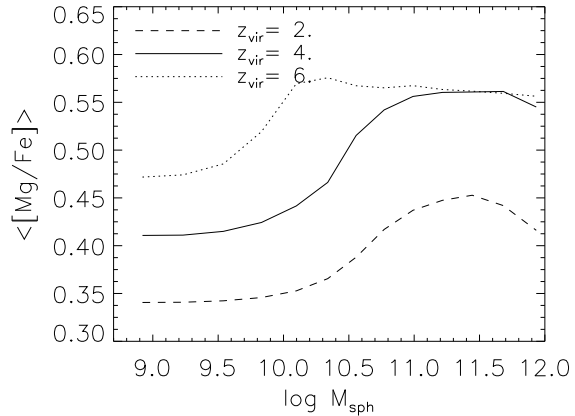


Fig. 9.— Mean Mg/Fe abundance ratio as a function of the present-day stellar mass for the usual 3 values of z_{vir} .

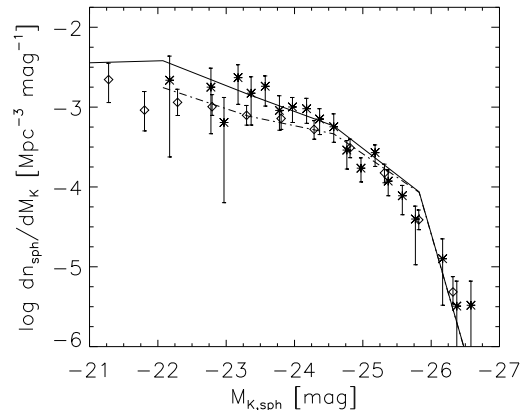


Fig. 10.— Predicted K-band local luminosity function of massive spheroids (solid line) compared with observational determinations by Kochanek et al. (2001; diamonds) and Huang et al. (2003; stars). The dot-dashed line shows the predicted local luminosity function of early-type galaxies only, i.e. after subtracting from the global luminosity function of spheroids the contributions of bulges of Sa and Sb galaxies (see text).

This 2-column preprint was prepared with the AAS L^AT_EX macros v5.0.

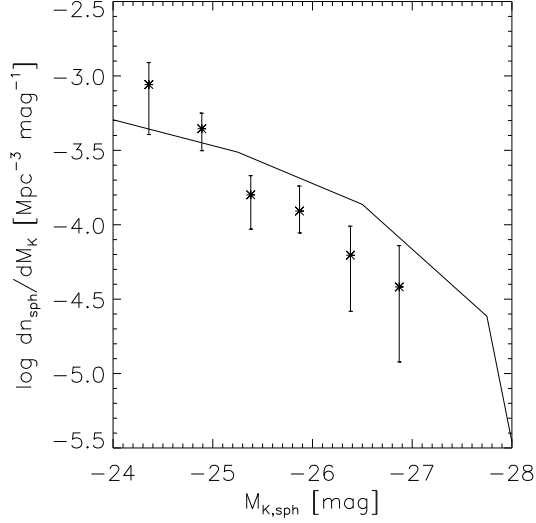


Fig. 11.— Predicted K-band luminosity function of massive spheroids at $z = 1.5$ compared with observational determination by Pozzetti et al. (2003).

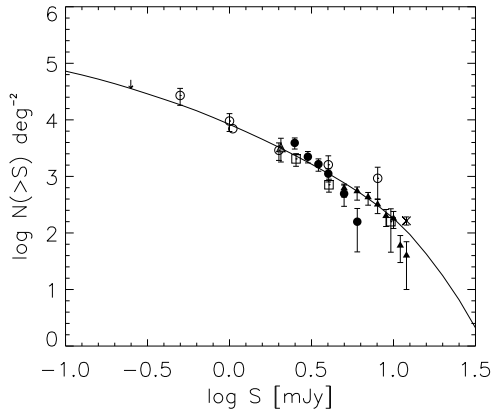


Fig. 12.— Predicted 850 μm extragalactic counts compared with SCUBA counts by Blain et al. (1999, open circles), Hughes et al. (1998, star and triangles), Barger et al. (1999, open squares), Eales et al. (2000, filled circles), Chapman et al. (2002, filled triangle), and Borys et al. (2002, filled squares).

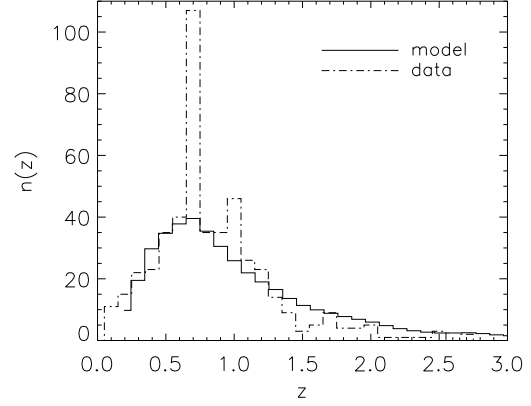


Fig. 13.— Predicted redshift distribution of galaxies brighter than $K = 20$ compared with the results of the K20 survey (Cimatti et al. 2002b).

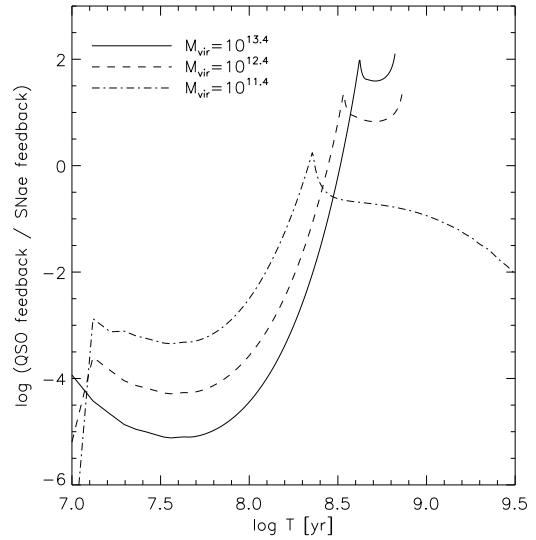


Fig. 14.— Ratio between the mass ejected from the galaxy per unit time by the feedback of the QSO and by that of SNaE.

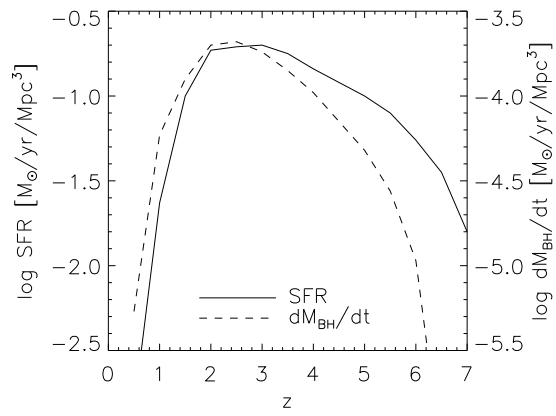


Fig. 15.— Predicted star formation in spheroids and BH mass accretion rates per unit volume as a function of redshift.